Blind benchmarking of seven longitudinal tensile failure models for two virtual unidirectional composites

C. Breite, A. Melnikov, A. Turon, A.B. de Morais, F. Otero, F. Mesquita, J. Costa, J.A. Mayugo, J.M. Guerrero, L. Gorbatikh, L.N. McCartney, M. Hajikazemi, P.P. Camanho, R.P. Tavares, S.V. Lomov, S. Pimenta, W. Van Paepegem, Y. Swolfs

PII: S0266-3538(20)32347-2

DOI: https://doi.org/10.1016/j.compscitech.2020.108555

Reference: CSTE 108555

To appear in: *Composites Science and Technology*

Received Date: 3 September 2020

Revised Date: 5 November 2020

Accepted Date: 8 November 2020

Please cite this article as: Breite C, Melnikov A, Turon A, de Morais AB, Otero F, Mesquita F, Costa J, Mayugo JA, Guerrero JM, Gorbatikh L, McCartney LN, Hajikazemi M, Camanho PP, Tavares RP, Lomov SV, Pimenta S, Van Paepegem W, Swolfs Y, Blind benchmarking of seven longitudinal tensile failure models for two virtual unidirectional composites, *Composites Science and Technology*, https://doi.org/10.1016/j.compscitech.2020.108555.

Christian Breite: Conceptualization, Methodology, Software, Formal analysis, Investigation, Writing - Review & Editing

Arsen Melnikov: Conceptualization, Methodology, Software, Formal analysis, Investigation, Writing - Review & Editing

Albert Turon: Writing - Review & Editing, Supervision

Alfredo B. De Morais: Software, Investigation, Writing - Review & Editing

Fermin Otero: Software, Writing - Review & Editing

Francisco Mesquita: Conceptualization, Methodology, Software, Investigation, Writing - Review & Editing

Josep Costa: Writing - Review & Editing, Supervision

Joan A. Mayugo: Writing - Review & Editing, Supervision

José Manuel Guerrero: Software, Investigation, Writing - Review & Editing

Larissa Gorbatikh: Writing - Review & Editing, Supervision

Mohammad Hajikazemi: Software, Investigation, Writing - Review & Editing

Neil McCartney: Software, Investigation, Writing - Review & Editing

Pedro P. Camanho: Writing - Review & Editing, Supervision

Rodrigo Tavares: Software, Investigation, Writing - Review & Editing

Soraia Pimenta: Conceptualization, Methodology, Software, Investigation, Writing - Review & Editing

Stepan V. Lomov: Writing - Review & Editing, Supervision

Wim Van Paepegem: Investigation, Writing - Review & Editing, Supervision

Yentl Swolfs: Conceptualization, Methodology, Software, Formal analysis, Writing - Original Draft, Writing - Review & Editing, Visualization, Supervision

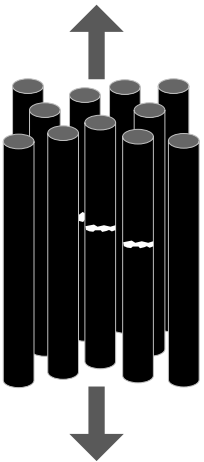

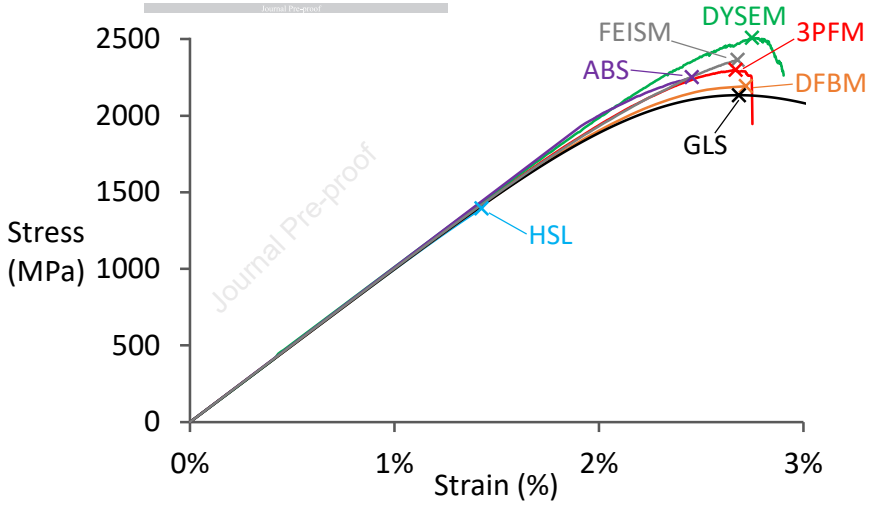
Journal Pre-proof
2500
2000
1500
1000
500
0
Stress (MPa)
0%
1%
2%
3%
Strain (%)
DYSEM
FEISM
3PFM
ABS
DFBM
GLS
HSL
Journal Pre-proof

Blind benchmarking of seven longitudinal tensile failure models for two virtual unidirectional composites

C. Breite[1], A. Melnikov[1], A. Turon[2], A.B. de Morais[3], F. Otero[4], F. Mesquita[1], J. Costa[2], J.A. Mayugo[2], J.M. Guerrero[2], L. Gorbatikh[1], L. N. McCartney[5], M. Hajikazemi[6], P.P. Camanho[4,7], R.P. Tavares[4,7], S.V. Lomov[1], S. Pimenta[8], W. Van Paepegem[6], Y. Swolfs[1]

[1]Department of Materials Engineering, KU Leuven, Kasteelpark Arenberg 44 box 2450, 3001 Leuven, Belgium
[2]AMADE, Polytechnic School, University of Girona, Campus Montilivi s/n, E-17003 Girona, Spain
[3]Department of Mechanical Engineering, RISCO research unit, University of Aveiro, Campus Santiago, 3810-193 Aveiro, Portugal
[4]INEGI, Rua Dr. Roberto Frias, 400, 4200-465 Porto, Portugal
[5]Department of Engineering, Materials & Electrical Science, National Physical Laboratory, Teddington, Middlesex TW11 0LW, United Kingdom
[6]Department of Materials, Textiles and Chemical Engineering, Faculty of Engineering and Architecture, Ghent University, Technologiepark Zwijnaarde 46, Ghent, Belgium
[7]DEMec, Faculdade de Engenharia, Universidade do Porto, Rua Dr. Roberto Frias, 4200-465 Porto, Portugal
[8]meComposites, Department of Mechanical Engineering, Imperial College London, South Kensington Campus, London SW7 2AZ, United Kingdom

Keywords: B. Strength, B. Mechanical properties, C. Computational mechanics, C. Stress concentrations, Longitudinal tensile failure

Abstract

Many models for prediction of longitudinal tensile failure of unidirectional (UD) composites have been developed in the last decades. These models require significant assumptions and simplifications, but their consequences for the predictions are often not clearly understood. This paper therefore presents a blind benchmark of seven different models applied to two virtual materials. Reliably capturing the localisation of stress concentrations was vital in predicting the effect of matrix stiffness and strength on composite failure strain and strength as well as fibre break and cluster development. Although the models have different assumptions regarding stress redistributions around fibre breaks, the 2-plet (clusters of two fibre breaks) development was similar. Distance-based criteria were shown to be inadequate for monitoring cluster development. The discussions provide detailed insight into how the model assumptions are linked to the differences in the predictions.

1 Introduction

Fibre-reinforced composites offer a high specific stiffness and strength, and are therefore increasingly being used in high-performance and consumer applications. However, many applications are heavily overdesigned due to a lack of (1) fundamental

understanding of their failure development and (2) reliable predictive models for mechanical properties. This has been emphasised by three World-Wide Failure Exercises [1-3]. Admittedly, the ambitions of these exercises were set very high: predicting the damage development and failure of multidirectional laminates under multiaxial loading and comparing it against difficult-to-perform and non-standardised experiments.

A simpler scenario is longitudinal tension of unidirectional (UD) composites; one could even argue it is the simplest possible scenario for composites. This, however, does not imply that reliable prediction of longitudinal tensile strength and failure strain is a simple task. The modelling efforts in this regard started in the 1960's, 1970's and 1980's [4-8], and became very active in the last decade [9-19]. All models are essentially based on the same two principles:

1. The fibre strength scatter follows a Weibull distribution;
2. When a fibre breaks, it locally loses its longitudinal load transfer capability, which leads to stress concentrations on the surrounding fibres.

The implementation and assumptions of the models, however, vary significantly [20]. Nevertheless, many models reported a good match with experimental strengths or failure strains within a deviation of about 15% [9,14,16,17,21,22]. This good match should, however, be interpreted with care, as it strongly depends on the input parameters. Table 1 illustrates that for one particular carbon fibre type (T700 or T700S) characterised by one particular type of test (single fibre tensile test), the Weibull parameters can vary significantly. The Weibull modulus ranges from 3.23 to 5.39, and the predicted composite strength (based on the global load sharing (GLS) model of Hui et al. [23]) varies strongly between 2810 MPa and 4730 MPa (see Table 1). Given the large effect of just one input data, it is unrealistic to consistently predict the tensile strength within 15% of experimental results; some confirmation bias [24] likely occurred.

Table 1: Collection of Weibull data from single fibre tensile tests on T700 or T700S carbon fibres and predicted composite strength from the literature. The predicted composite strength is based on the global load sharing model of Hui et al. [23], as implemented in Swolfs et al. [25].

Source	Year	Number	Weibull scale	Weibull	Reference	Predicted GLS
Feih et al. [26]	2012	30+	5315	5.14	20	3270
Xiao et al. [27]	2013	30+	-	5.39	20	-
Deng et al. [28]	1998	20+	7700	3.5	10	4350
			6200	5.0	20	3750
			6200	4.0	30	4400
			6000	3.7	40	4730
			5800	4.0	50	4620
Mesquita et al.	2019	217	4710	3.94	12	2950
Joannès et al. [30]	2020	30	4190	3.23	30	3630
Islam et al. [31,32]	2020	120	5720	3.55	4	2810
		135	5160	3.50	20	3720
		350	4630	3.48	30	3750

The strong variations highlighted in Table 1 make it challenging to objectively compare models based on published papers. A first benchmark was therefore initiated, and the results thereof were published in 2018 [33]. This benchmark dealt with longitudinal tensile failure of unidirectional (UD) composites, and included three modelling participants (KU Leuven [9-12], MINES ParisTech [21] and Imperial College London [13,14]) and one experimental participant (University of Southampton [9,21]). Even when the input parameters were the same, predictions from the three different models still differed significantly: the largest predicted tensile strength for a T800/M21 composite was 50% higher than the lowest prediction. The deviation from the experimentally measured failure strain reached 59%, and the fibre break and cluster development showed even larger differences. A number of significant issues were highlighted by this benchmark:

1. The underlying modelling approaches and assumptions were so different that it was difficult to pinpoint the precise origins of the differences in predictions.
2. The actual input parameters were not characterised in the study. Firstly, literature data were used for the Weibull distribution for fibre strength, and using different distribution parameters would have changed the results significantly (see Table 1). Secondly, the properties of the matrix were estimated, as the neat resin was not available for characterisation.
3. The experimental validation data based on in-situ synchrotron computed tomography were limited: only three scans were performed at relevant load levels

on the same specimen. Moreover, all scans were performed while the specimen was held at constant displacement, a procedure that may have introduced artefacts due to stress relaxation.

4. Only three models participated, even though there are many more models in the literature.

There is hence a clear need for a new benchmark with more reliable experimental input and validation data, more modelling participants and a more detailed analysis and interpretation. This paper takes a first step in this direction by performing a truly blind comparison of model predictions for two virtual materials. This is the most reliable approach to objectively assess the effect of different modelling approaches and assumptions, as it is not affected by experimental difficulties. The goal of this paper is therefore not to establish the best model, but rather to provide an objective comparison between the participating models, to better understand their key differences and to identify the assumptions with the greatest impact on the predictions.

After describing the general setup of the benchmark, the main model features will be described and compared. Then, the two modelled cases will be explained, followed by the presentation and detailed discussion of the results.

2 Setup of the benchmark

The benchmark was initiated by four partners (KU Leuven, Imperial College London, MINES ParisTech and University of Southampton). They jointly set up the draft instructions for the benchmark and invited participants. All nine partners that accepted the initial invitation were given the chance to suggest changes to the instructions. Once all participants agreed on the instructions, the instructions were made publically available [34], so that future researchers can build further upon this benchmark. Six of the nine participants provided results to the benchmark described in this paper (see Table 2). Once all results were submitted, an in-person meeting was organised to discuss the results and agree upon the next steps. One of the conclusions from this meeting was to add predictions from a seventh model, which was the global load

sharing model developed by Hui et al. [23]. One of the participants (ABS, see Table 2) was allowed to submit new results for the "stiff/strong" matrix case (see section 4 Description of the two cases), as the initial ABS results for that case included fibre-matrix debonding. However, modelling of fibre-matrix debonding was excluded from the benchmark, and therefore new results without fibre-matrix debonding were generated. This was the only change relative to the initial ABS results.

3 Key features of the models

A total of seven model predictions will be presented. Table 2 gives the names, acronyms and key references describing the models. Since all of these models have already been thoroughly described in the literature, the details will not be presented here. To properly understand and interpret the results, however, it is vital to highlight the main assumptions, limitations, benefits and drawbacks of the models. To facilitate this, Table 3 provides an overview of the key features of each model. SCF in this table stands for Stress Concentration Factor, WOW for Weibull of Weibull and PLAW for Power Law Accelerated Weibull. Cluster size refers to the number of fibres in a cluster.

Table 2: The seven models used in the present benchmark, their acronyms and some key references.

Full name	Acronym	Institution	References
3D progressive failure model	3PFM	University of Girona (Spain)	[15,16]
Analytically based-strength simulation	ABS	National Physical Laboratory (UK) and Ghent University (Belgium)	[35,36]
Dispersed fibre breaks model	DFBM	University of Aveiro (Portugal)	[22]
Dynamic spring element model	DYSEM	University of Porto (Portugal)	[17-19]
Finite element-imposed stress model	FEISM	KU Leuven (Belgium)	[9-12]
Global load sharing	GLS	Cornell University (USA)	[23]
Hierarchical scaling law	HSL	Imperial College London (UK)	[13,14]

A few differences are particularly important:

- Three models are probabilistic in nature, as they calculate the failure probabilities for any given stress or strain level: HSL, DFBM and GLS. The other four models use Monte Carlo simulations.
- Not all models used the same matrix behaviour: FEISM, DFBM and DYSEM used the recommended linear elastic-perfectly plastic behaviour, whereas HSL, GLS and 3PFM simplified this to perfectly plastic and ABS to linear elastic in the normal direction and perfectly plastic in the shear direction.

Table 3: Overview of the key features of the seven participating models.

Feature		3PFM	ABS	DFBM	DYSEM	FEISM	GLS	HSL
Material response	Elastic properties of fibre	Linear elastic up to failure, isotropic. Non-linear elastic behaviour can be incorporated in an approximate manner.	Linear elastic, transversely isotropic.	Linear-elastic, no consideration of anisotropy.	Linear elastic, isotropic. Non-linear elastic behaviour can be incorporated in an approximate manner.	Linear elastic, transversely isotropic. Non-linear elastic behaviour can be incorporated in an approximate manner.	Linear elastic, no consideration of anisotropy.	Linear-elastic, no consideration of anisotropy.
	Fibre strength distribution	Standard implementations for unimodal, bimodal and PLAW available, but others can easily be plugged in.	At the moment, unimodal distribution only, but others can easily be plugged in. Strength values smaller than half of the mean or larger than two standard deviations above it are rejected.	At the moment, unimodal distribution only. Equations need to be reworked for other Weibull distributions.	Standard implementations for unimodal, bimodal, WOW and PLAW available, but others can easily be plugged in.	Standard implementations for unimodal, bimodal and PLAW are available, but others can easily be plugged in.	Unimodal distribution only	At the moment, unimodal distribution only. Equations need to be reworked for other Weibull distributions.
	Matrix	Perfectly plastic (elastic also possible)	Linear elastic (perfectly plastic in shear if debonding would be present)	Linear elastic-perfectly plastic	Linear elastic-perfectly plastic. More complex behaviours can be used.	Linear elastic-(nearly) perfectly plastic. More complex behaviours can be used.	Perfectly plastic	Perfectly plastic in shear, considered in combination with the interface.
	Interface	Perfect bonding assumed. In principle possible to add this effect approximately.	Perfect bonding assumed here, but can be taken into account.	Perfectly plastic in shear, considered in combination with the matrix.	Perfect bonding assumed. Prepared for taking debonding into account but not done yet.	Perfect bonding assumed. In principle possible to add this effect approximately.	Perfectly plastic in shear, considered in combination with the matrix.	Perfectly plastic in shear, considered in combination with the matrix.
Fibre packing type		Random (regular also possible)	Hexagonal	Hexagonal	Random (regular also possible)	Random (regular also possible)	Not relevant	Square (hexagonal also possible)
Stress concentrations	Near individual fibre breaks	Analytical function calibrated with FE simulations and a spring element model.	Analytical model based on equilibrium equations, interface continuities and stress-strain equations, load shared by six nearest neighbours	Shear lag along the fibres, load shared by all remaining fibres	Actual stress redistribution from equilibrium equations, including dynamic stress concentrations.	3D FE model to capture the entire stress redistribution. Modelled at 2% macroscopic strain.	Shear lag along the fibres, load shared by all remaining fibres	Shear lag, considering that all excess load is carried by one neighbouring fibre.
	Near multiple fibre breaks	Linear superposition; the model captures the increase in ineffective length with cluster size, but only if the breaks are located at the same plane.	Load shared by all nearest neighbours to the cluster.	Not relevant	Superposition not necessary. The model captures the increase in ineffective length with cluster size.	Enhanced superposition principle, which is accurate in plane. The increase in ineffective length is not captured, but addressed in ongoing work.	Shared by all fibres	Shear-lag, considering that all excess load is carried by one neighbouring cluster of the same size as the broken cluster.
Clusters of fibre breaks	Definition	Distance-based criterion. Can be changed according to the specifications	Distance-based criterion. Can be changed according to the specifications	Cannot be tracked.	Distance-based criterion. Can be changed according to the specifications	Distance-based criterion. Alternative criterion based on the % of SCF also available.	Cannot be tracked.	A cluster is defined by fibre breaks/sub-broken-clusters with interacting recovery regions.
	Cluster sizes	Any size is possible	Any size is possible	Not applicable	Any size is possible	Any size is possible	Cannot be tracked.	1, 2-3, 4-7, …
	Coplanarity	Can monitor coplanarity, but does not enforce it.	One cell covers more than one ineffective length, which prevents stress concentrations from affecting cells in other layers.	Does not consider clusters of fibre breaks, but the co-planar breaks condition can be enforced	Can monitor coplanarity, but does not enforce it.	Can monitor coplanarity, but does not enforce it.	Cannot be tracked.	Does not impose co-planar breaks to calculate failure probabilities, but does assume co-planar breaks to model stress fields near broken clusters
Matrix contribution to composite stress calculation		Linear elastic matrix contribution included	Linear elastic matrix contribution included	Not included	Not included	Linear elastic-perfectly plastic matrix contribution included	Perfectly plastic axial matrix contribution included	Not included
Simulation type		Monte Carlo	Monte Carlo	Probabilistic	Monte Carlo	Monte Carlo	Probabilistic	Probabilistic
Information regarding pre-calculations		Generation of the random packing is run prior the start of the simulation.	No pre-calculations needed	No pre-calculations needed	Generation of the random packing is run prior the start of the simulation.	FE simulations are needed for a non-standard carbon fibre or new matrix behaviour. Basic library of fibre-matrix combinations is available. Generation of the random packing is run prior the start of the simulation.	No pre-calculations needed	No pre-calculations needed
Determination of final failure		When either a load drop of 10% is detected or all fibres in a cross-section are broken.	When just one axial layer of elements has failed completely after the system becomes unstable due to an avalanche of fibre breaks. Other criteria are available.	By the maximum stress that the representative volume element can withstand	When the stress drops below 90% of the maximum stress.	When an avalanche of fibre breaks occurs without any increase in macroscopic strain. The model captures this through a rising number of fibre breaks per iteration for the same strain increment.	By the maximum stress.	When the bundle cannot carry any additional load.

- The stress concentrations near individual fibre breaks are captured via Finite Element (FE) or FE-like calculations (FEISM, DYSEM), shear-lag (HSL, DFBM, GLS) or analytical functions (3PFM, ABS). Compared to the other models, the stress concentrations in HSL are very high (100%) because the load from the broken fibre is fully shed on the nearest neighbour (i.e. highly localised load sharing). ABS assumes that the stress concentrations are carried by the surviving nearest neighbours only. The stress concentrations are very low in DFBM and GLS, as they are spread over the whole bundle (global load sharing).
- HSL and DYSEM inherently capture the increase in ineffective length with fibre break cluster size, whereas 3PFM only captures this effect for coplanar cluster. FEISM and ABS do not include this feature, and clusters are not relevant in DFBM and GLS.
- DYSEM is the only model capturing dynamic stress concentrations.
- ABS used the recommended radial distance criterion, but a more generous axial distance criterion when defining clusters. Their axial criterion enabled fibre breaks in one of the nearest neighbours that are one axial layer away (=500 µm) to be part of the same cluster.

4 Description of the two cases

The main goal of the two cases described here was to deliberately make them as blind as possible. It was therefore decided to use virtual rather than real materials, so that the modellers did not have any expectation about solutions a priori. Two distinct cases were modelled where only the matrix stiffness and shear yield stress were altered (see Table 4). These two cases will be referred to as the “compliant/weak” matrix and “stiff/strong” matrix cases. They enable a fair comparison of the effect of matrix behaviour on predictions. The matrix was assumed to be linearly elastic-perfect plastic, and no interface debonding or matrix cracking was allowed to occur. These restrictions enabled a more objective comparison of the models. The fibre behaviour was assumed to be

linear elastic and isotropic, and fibre strength was assumed to follow a unimodal Weibull distribution (see Table 4).

Table 4: Fibre and matrix properties, as well as geometric parameters of the composite to be modelled.

		"Compliant/weak"	"Stiff/strong"
Fibre	Young's modulus (GPa)	200	
	Poisson's ratio (-)	0.2	
	Radius (µm)	6	
	Weibull scale parameter (MPa)	4000	
	Weibull modulus (-)	4	
	Reference gauge length (mm)	10	
Matrix	Young's modulus (GPa)	1	5
	Poisson's ratio (-)	0.3	
	Shear yield stress (MPa)	20	100
Composite bundle	Fibre volume fraction (-)	50%	
	Length (mm)	4	
	Number of fibres (-)	2000	
	Cross-sectional shape	Unspecified	

For models where this is relevant (FEISM, 3PFM and DYSEM), an element length equal to the fibre diameter (12 µm) was prescribed. The type of packing (random or regular) could be freely chosen, as its effect on the predictions is anyway minor [10]. Residual stresses were ignored to make the comparison easier and because debonding was not included. The participants were recommended to use a cluster criterion based on distance: all fibre breaks within an axial distance of 330 µm ("compliant/weak" matrix) or 78 µm ("stiff/strong" matrix) and a radial centre-to-centre distance of 24 µm of each other were considered part of the same cluster. These distances were based on FE models of a single fibre break in a hexagonal packing at an applied strain of 2% [12], which revealed where stress concentrations were likely going to be significant. HSL did not follow this criterion, as it has a built-in cluster definition [14]. ABS adhered to the radial distance criterion, but used a different criterion in the axial direction: a fibre break in one of the nearest neighbours in the plane above or below another fibre break would be considered as part of the same cluster. This criterion is significantly more expansive than the recommended one, especially for the "stiff/strong" matrix case, as the planes in ABS are 500 µm apart.

For the models based on Monte Carlo simulations (see Table 3), at least 10 and preferably 50 runs were requested for each of the cases. ABS and DYSEM submitted 10 runs, whereas 3PFM and FEISM submitted 50 runs. A total of 7 outputs were requested:

1. The time required for each run;
2. A representative or averaged stress-strain diagram;
3. The strength (defined as the maximum longitudinal stress sustained by the composite) and the failure strain (defined as the average longitudinal strain of the composite at the point of maximum stress) for each run.
4. The average fibre break density as a function of macroscopic strain;
5. The average number of i-plets (clusters of size i) as a function of macroscopic strain;
6. The average size of the largest cluster (number of fibre breaks/cluster) as a function of macroscopic strain;
7. The average cluster height and average standard deviation of the axial distance of every fibre break from its cluster centre as a function of macroscopic strain.

The probabilistic models in Table 3 did not require multiple runs, and therefore submitted only the statistical expected values (i.e. mathematical expectations). HSL also supplied standard deviations, which was not possible for DFBM and GLS. The averages were calculated over all Monte Carlo simulations up to the average failure strain.

The first and last outputs merit some further explanation. The time required for each simulation was provided alongside information on the type CPU and the number of cores. The computational times were normalised based on the “Average CPU Mark” on www.cpubenchmark.net and the number of cores that were used. This was done in such a way that the FEISM computational time had a normalisation factor of 1. It should be noted that the percentage per core that was actually used was not taken into account. The cluster height and standard deviation information were requested to characterise the coplanarity of the clusters. This approach provides more detailed information than a simple distinction between coplanar and diffuse clusters, as was used in past research [9]. All reported scatter values are the standard deviations.

5 Results

5.1 Basic results

Figure 1 shows the normalised computational time per simulation. An important difference is that four models (FEISM, 3PFM, DYSEM and ABS) run Monte Carlo simulations, whereas HSL, DFBM and GLS do not. HSL predicts the failure distributions [14], whereas DFBM and GLS have a deterministic outcome. The computational time for DFBM could not even be recorded as these calculations are done almost instantaneously in an Excel sheet. The computational times vary by more than 5 orders of magnitude, with HSL being the fastest and DYSEM being the slowest model. DYSEM solves the full dynamic equilibrium equations with an explicit time integration scheme, whereas HSL is fully analytical. The "stiff/strong" matrix case required more computational time for the FEISM, 3PFM, DYSEM and ABS models, whereas this barely affected GLS and HSL. It should be noted that the models that used random fibre packings (FEISM, 3PFM and DYSEM) also required additional time to generate those packings. FEISM, in addition, requires FE models to set up a library of stress concentrations (see Table 3).

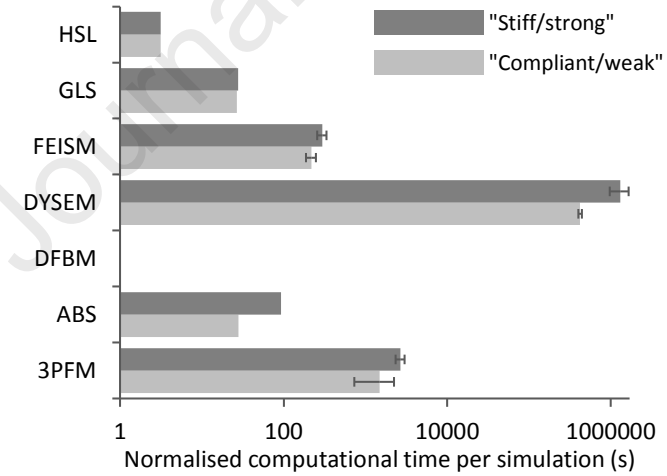

Figure 1: Computational time per simulation, normalised based on the "Average CPU Mark" and the number of cores that were used. Note the use of a logarithmic x-axis. HSL, GLS and DFBM are probabilistic models and therefore only needed to be run once. The error bars represent the standard deviation, which was zero for the probabilistic models. ABS only tracked the total run time for all simulations, and hence no standard deviation could be calculated.

Figure 2 displays the stress-strain diagrams of the composites, Figure 3 the failure strain and strength values and Figure 4 the fibre break density evolution. Figure 2 and Figure 3 reveal that the "stiff/strong" matrix case always leads to a larger strength and failure strain. HSL predicts notably lower failure strain and strength values than the other six models. Note that the DFBM and GLS results are size-independent, whereas the other

models would yield different failure strain and strength values for other model sizes [10,14,16,37]. The Weibull predictions in Figure 4 were calculated based on the Weibull failure probability for the given length of fibres present in the volume. These predictions serve as a reference case without any stress concentrations or stress recovery regions.

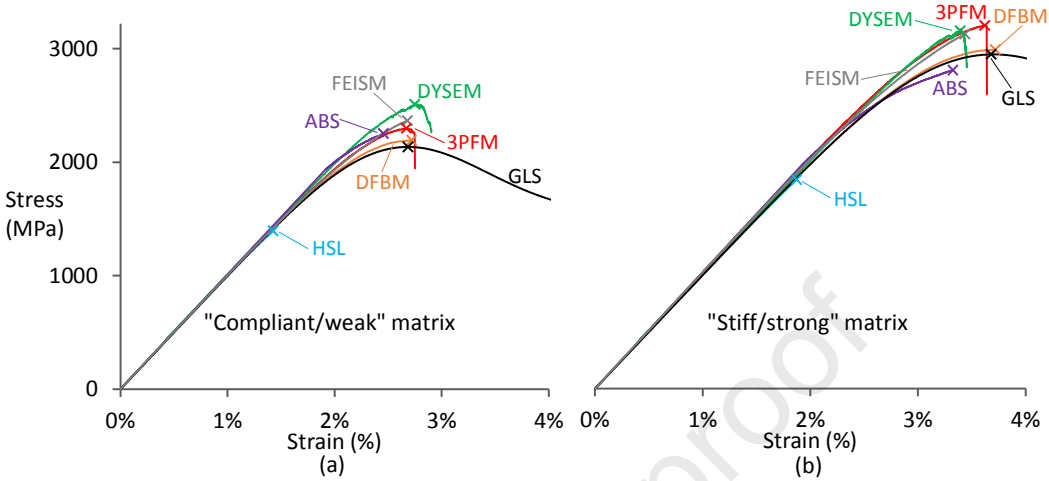

Figure 2: Representative stress-strain diagrams: (a) the "compliant/weak" matrix case and (b) the "stiff/strong" matrix case. The 'x' indicates the failure strain.

Figure 3: Failure predictions: (a) failure strain and (b) strength. The failure strain was calculated at the maximum stress point.

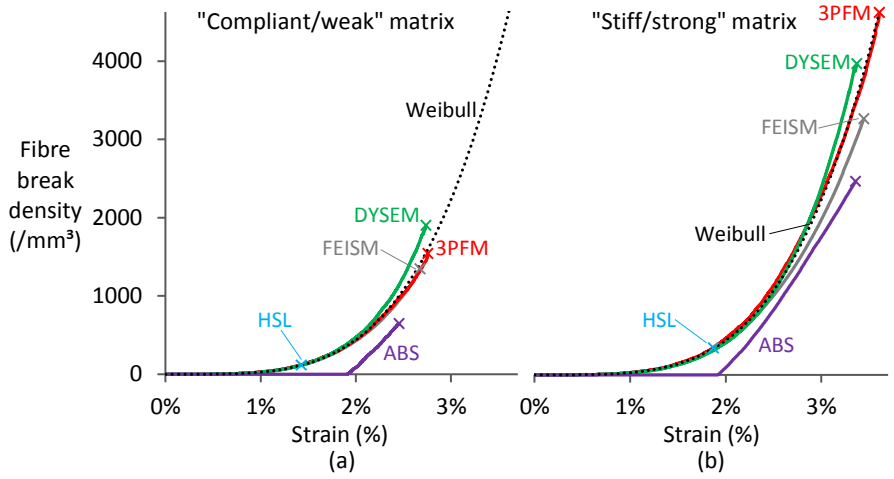

Figure 4: Average fibre break density as a function of macroscopic strain: (a) "compliant/weak" matrix case, and (b) "stiff/strong" matrix case. The DFBM and GLS model are not included, as they only predict fibre break densities indirectly. For Monte Carlo simulations, these data were averaged over all simulations up to the average failure strain; for HSL, these data correspond to the expected values. The 'x' indicates the failure strain.

Four of the five models (HSL, FEISM, DYSEM and 3PFM) predict similar initial fibre break density evolutions, which are in line with the Weibull predictions. This is expected, as the initial fibre break density is governed purely by the Weibull distribution rather than how the models handle stress concentrations. The ABS model is different from the other four models, since it does not allow fibre strength values that are smaller than half of the mean strength value. This leads to a later onset of fibre break development (see Figure 4).

5.2 Cluster development

More detailed insight can be gained from analysing the cluster development. Unfortunately, the concept of clusters is not present in GLS and DFBM. HSL and ABS can both monitor cluster development, but not their coplanarity. HSL does not impose co-planar breaks to calculate failure probabilities, but does assume co-planar breaks to model stress fields near broken clusters (see Table 3). ABS deliberately uses an element length (500 µm) that is longer than the ineffective length. The stress concentrations created by a fibre break are therefore confined to the same layer of elements, making ABS unable to track coplanarity.

Figure 5 and Figure 6 display the evolution of 2-plet and 3-plet density (two and three fibre breaks organised in a cluster), respectively, as a function of macroscopic strain.

- FEISM, DYSEM and 3PFM are consistent in terms of 2-plet and 3-plet development (see Figure 5 and Figure 6).
- HSL is not able to distinguish between 2-plet and 3-plets, making the interpretation more complex. However, considering that 3-plet densities are significantly lower, the 2/3-plet densities predicted by HSL are not much higher than those predicted by FEISM, 3PFM and DYSEM.
- The “stiff/strong” matrix case leads to a later onset of 2-plet and 3-plet development, but a larger 2-plet and 3-plet density at the failure strain. This is true for all five models in Figure 6 apart from ABS, which shows similar development for both cases and a smaller final value for the “stiff/strong” matrix case.

- The models based on Monte Carlo simulations can predict a maximum in the 2-plet and 3-plet density followed by a decrease: 3PFM, DYSEM and FEISM for the "compliant/weak" case and ABS for the "stiff/strong" case. This is attributed to these small clusters growing to larger clusters faster than the formation of new 2-plets and 3-plets.

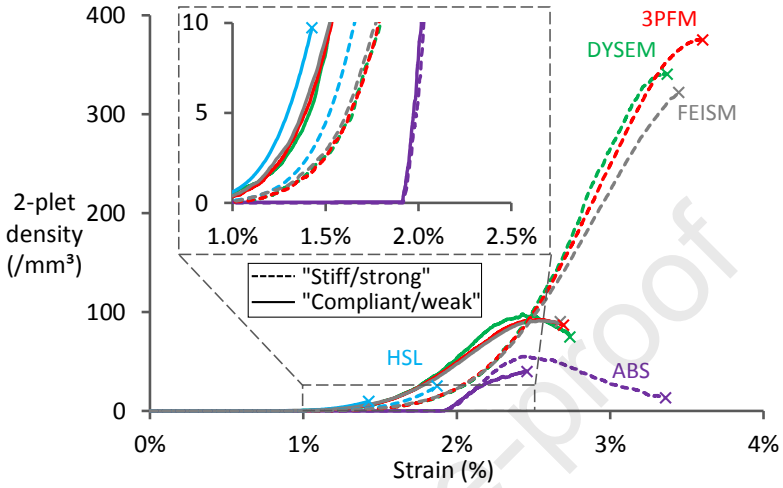

Figure 5: 2-plet density as a function of macroscopic strain: solid lines for the "compliant/weak" matrix case and dashed lines for the "stiff/strong" matrix case. For HSL, the line represents clusters with 2-3 fibre breaks. For Monte Carlo simulations, these data were averaged over all simulations up to the average failure strain; for HSL, these data correspond to the expected values. The 'x' indicates the failure strain.

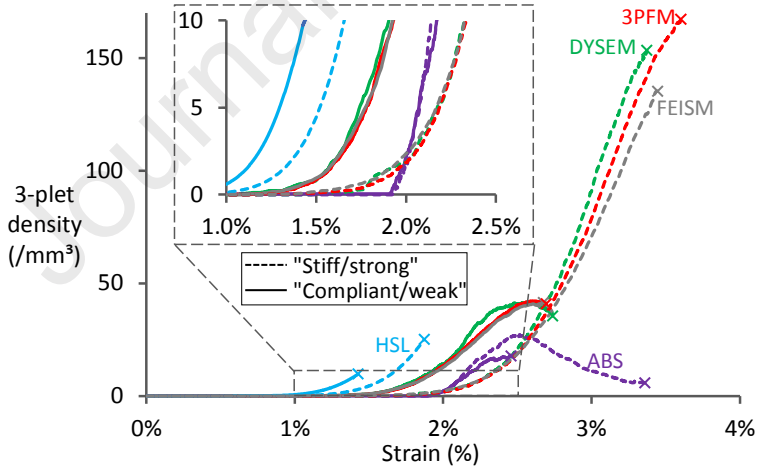

Figure 6: 3-plet density as a function of macroscopic strain: solid lines for the "compliant/weak" matrix case and dashed lines for the "stiff/strong" matrix case. For HSL, the line represents clusters with 2-3 fibre breaks. For Monte Carlo simulations, these data were averaged over all simulations up to the average failure strain; for HSL, these data correspond to the expected values. The 'x' indicates the failure strain.

Figure 7 displays the average largest cluster size (rounded to the nearest integer) as a function of macroscopic strain.

- Four of the five models (FEISM, HSL, DYSEM and 3PFM) predict nearly the same onset strain for fibre break development (0.3-0.4%, see insets in Figure 7), as this is

governed by the Weibull distribution. As shown in Figure 5 and Figure 7, the same applies to the 2-plet density.

- Once the average largest cluster size grows larger than a 3-plet, however, the average largest cluster size starts increasing more rapidly for HSL than for the other models. This is attributed to the higher stress concentrations in HSL compared to the other models.
- DYSEM diverges more in terms of largest cluster development (see Figure 7). This occurs because it captures dynamic stress concentrations, making it more likely to trigger larger clusters [38].
- ABS predicts a different onset because it removes the weakest elements for the Weibull distribution (see Table 3).
- ABS predicts an average largest cluster size of 4233 for the "stiff/strong" matrix case, which is much larger than any of the other models. This is because their axial cluster criterion enabled fibre breaks in adjacent axial layers to link up to form clusters, despite being separated by 500 µm. The same fibre can therefore break multiple times with those breaks being considered part of the same cluster. This criterion in ABS was therefore more expansive than in the other models.

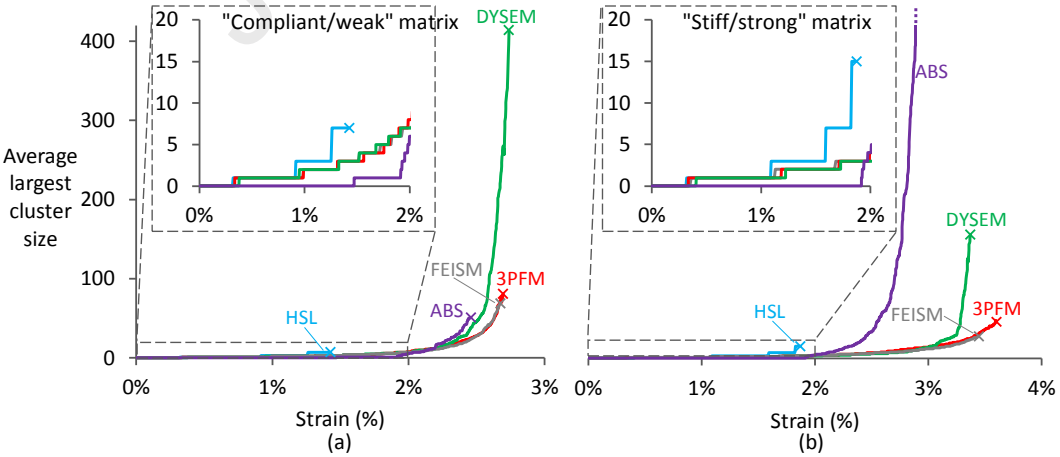

Figure 7: Average largest cluster size as a function of macroscopic strain for the (a) "compliant/weak" matrix case and (b) "stiff/strong" matrix case. For Monte Carlo simulations, these data were averaged over all simulations up to the average failure strain; for the HSL, these data correspond to the expected values. ABS goes up to 4233 for the "stiff/strong" matrix case. The 'x' indicates the failure strain.

Figure 8 characterises the coplanarity of the clusters using two different parameters: average cluster height and standard deviation of the 3-plets. The three models predict similar evolutions of both parameters, which are much smaller for the "stiff/strong"

matrix case (dashed lines) than for the "compliant/weak" matrix case (solid lines). 3PFM assumes perfectly plastic matrix behaviour, whereas DYSEM and FEISM assume linear elastic-perfectly plastic. This implies that the stress recovery in 3PFM occurs over a shorter length, and that stress concentrations are more local. This is more pronounced in the "stiff/strong" case, where it leads to smaller cluster height standard deviations than for DYSEM and FEISM.

The average cluster height and the cluster height standard deviation for 3-plets yield very similar evolutions. The main differences between both parameters lie in their behaviour for larger clusters, although this is not shown here. While the average cluster height for 5-plets is about 60-70% larger than for 3-plets, this increase is limited to just 24-43% for the cluster standard deviation, depending on the model and case. The cluster standard deviation is therefore easier to compare between different sources, as it depends less on cluster size than the cluster height.

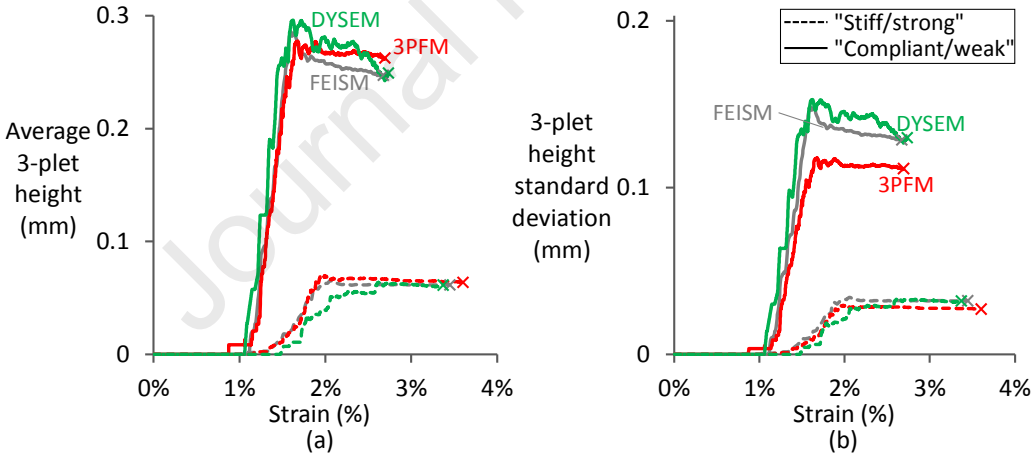

Figure 8: The degree of coplanarity of the 3-plets as measured by two different parameters: (a) average 3-plet height and (b) 3-plet height standard deviation. The solid lines represent the "compliant/weak" matrix case and the dashed lines represent the "stiff/strong" matrix case. These data were averaged over all simulations up to the average failure strain, and the 'x' indicates the failure strain.

6 Discussion

The higher computational time (see Figure 1) for the "stiff/strong" matrix in the Monte Carlo-based models (FEISM, 3PFM, DYSEM and ABS) is to a large extent explained by the higher failure strain (see Figure 3a) and fibre break density (see Figure 4), which thus requires more iterations to achieve equilibrium and final failure. The higher density in turn is linked to the fact that a stiffer and stronger matrix yields more localised stress

concentrations, both radially and axially. The axial localisation delays cluster development and hence final failure.

The slight differences in the initial slope of the stress-strain curves in Figure 2 are attributed to some models (DFBM, DYSEM, HSL and GLS) ignoring the matrix contribution in the calculation of the composite stress (see Table 3). 3PFM and FEISM do take this contribution into account, and hence predict a stiffness that is 0.5% and 2.5% higher in the “compliant/weak” “and “stiff/strong” matrix case, respectively (see Figure 2b). ABS also takes into account the matrix contribution and predicts a stiffness that is 1% and 2.5% higher, respectively. The small difference with 3PFM and FEISM is because ABS uses a two-concentric cylinder model that also accounts for transverse constraints [39] (in contrast with linear rule-of-mixtures). However, this is not a major difference for the cases modelled here (nor for the most widely used fibre-reinforced composites), as the matrix contribution is small relative to the fibre contribution.

A remarkable difference between the models is the degree of non-linearity of the stress-strain curves (see Figure 2). The HSL predictions are the only ones that seem close to linear, whereas the other models show pronounced non-linearity. The predicted non-linearity originates from two features: (1) fibre breaks locally make the fibres less effective in transferring stress and (2) the matrix non-linearity under tension. The matrix non-linearity under tension should be negligible, as global matrix yielding only starts at a tensile strain of 3.46% for both cases and some models do not even include it (HSL, DFBM and DYSEM). The loss in stress transfer capability therefore strongly depends on the density of fibre breaks and clusters predicted by the model. For a proper comparison, the non-linearity needs to be plotted as a function of the fibre break density. Figure 9 plots the secant modulus relative to the initial secant modulus as a function of fibre break density. DYSEM’s stress-strain curve at low fibre break densities is not entirely linear due to a switch from the static to the dynamic version of the model. This is why its relative secant modulus rises above 100%.

The slope of Figure 9 is a measure of the decrease in stress transfer capability per broken fibre. In all five models, a stiffer and stronger matrix causes a significantly slower reduction in the relative secant modulus, although the relative secant modulus at the failure strain is not necessarily different. All models apart from FEISM show an acceleration in the loss of stiffness with increased fibre break density. This is primarily linked to the fact that the ineffective length grows with increased cluster size, which is a feature that is not captured by FEISM.

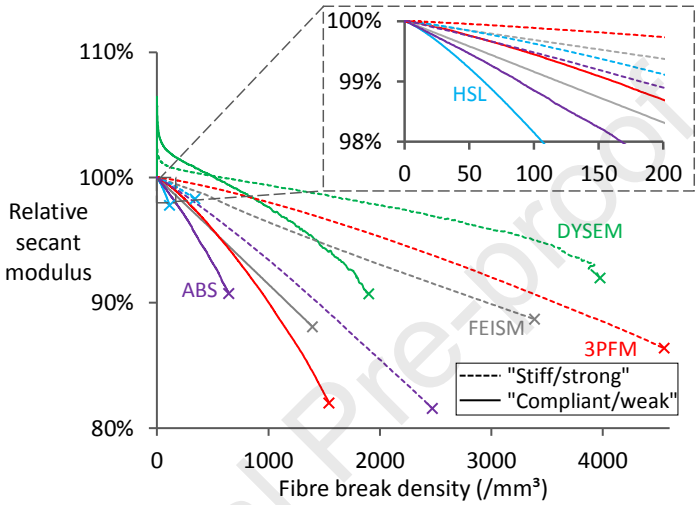

Figure 9: Evolution of the relative secant modulus as a function of fibre break density up to the average failure strain. Solid lines represent the "compliant/weak" matrix case and dashed lines represent the "stiff/strong" matrix case.

The modelling assumptions, and more specifically the way stress concentrations are implemented, only start mattering at higher fibre break densities. This is not only visible in the failure strain and strength predictions (see Figure 3) and fibre break density at the failure strain (see Figure 4), but also in the 2-plet, 3-plet and largest cluster development (see Figure 5 to Figure 7).

- HSL has the highest stress concentration (100% on the nearest neighbour, see Table 3), which is why it predicts specimen failure at the lowest failure strain and strength (see Figure 3); therefore, compared to all other models, HSL predicts that failure occurs at the lowest fibre break density.
- FEISM, 3PFM and DYSEM use lower and more spread out stress concentrations, which leads to higher failure strains and strengths than HSL (see Figure 3); consequently, these three models predict the highest fibre break density at the failure strain (see Figure 4).

- ABS sheds load to the nearest neighbours only, which implies that its level of stress concentrations lies in between those of HSL and those of FEISM, 3PFM and DYSEM. In addition, ABS considers a fibre strength distribution excluding the weakest tail (as explained in Table 3), and does not allow multiple fibre breaks to occur within one 500 µm element; this leads to a later onset of fibre failure and different fibre break density evolution compared to HSL, FEISM, 3PFM and DYSEM. Altogether, the differences in the treatment of stress concentrations and fibre strength distribution explain why ABS predicts failure strains similar to FEISM, 3PFM and DYSEM (see Figure 3) on the one hand, while it predicts intermediate fibre break density levels at the failure strain (see Figure 4).

The initial fibre break density evolution of 3PFM, DYSEM, FEISM and HSL matches well with the Weibull prediction (see Figure 4). This is because the assumptions regarding stress concentrations only start mattering when a significant fraction of the fibre breaks become part of a cluster. Closer to failure, DYSEM and FEISM start deviating from the Weibull predictions. DYSEM starts predicting a higher density, because of the presence of dynamic stress concentrations, whereas 3PFM and FEISM only capture static stress concentrations. FEISM, however, predicts a lower fibre break density than the Weibull prediction. While surprising at first, this is simply because the diagram is plotted as a function of strain rather than stress and the fact that fibre breaks introduce extra compliance. As a function of stress, the FEISM predictions are above the Weibull predictions. The 3PFM predictions are in line with the Weibull predictions for all strain levels and for both cases, likely because the described compliance and stress concentration effects happen to cancel out each other.

3PFM, DYSEM and FEISM predict that the average largest cluster size before failure for the “stiff/strong” matrix case is smaller than for the “compliant/weak” matrix case by 59%, 62% and 43%, respectively. In contrast, this average largest cluster size before

failure even increased from 7 in the "compliant/weak" matrix case to 15 in the "stiff/strong" matrix case for HSL. There are several competing effects here:

- In FEISM, 3PFM and DYSEM, the "stiff/strong" matrix case leads to in-plane and out-of-plane localisation of the stress concentrations, causing clusters to be smaller for a given applied strain. HSL does not capture the in-plane localisation for stiffer and stronger matrices, and always sheds the load to the nearest fibre or bundle, but does capture the out-of-plane localisation. Therefore, the argument of more local stress concentrations still applies to HSL, but to a lesser extent.
- The "stiff/strong" matrix leads to a stronger composite (see Figure 3b), which enables larger fibre break densities and cluster sizes and competes with the effect of more localised stress concentrations.
- The instructions recommended distance-based cluster criteria that were independent of the cluster size, which leads to underestimations of the size of large clusters. Larger clusters have a more widespread influence on their neighbors and produce a longer ineffective length [12,14,40,41], but these criteria failed to capture that feature. HSL's built-in cluster definition does automatically adjust the axial criterion for larger clusters.

The average largest cluster size before the failure strain was reached in ABS, was 50 and 4233 for the "compliant/weak" and "stiff/strong" case, respectively. However, the average largest cluster for the same strain level is always larger for the "compliant/weak" case, as this case creates stress concentrations on a larger volume and ABS's cluster criteria remained the same. The very large cluster size before failure in the "stiff/strong" matrix case is due to the expansive cluster criterion, enabling clusters in different axial layers to link up despite not influencing each other's stress fields.

The coplanarity analysis indicates that the clusters predicted by FEISM, 3PFM and DYSEM are far from coplanar (see Figure 8). The "compliant/weak" matrix case leads to a significantly lower coplanarity than the "stiff/strong" matrix case. This is related to the

shorter ineffective length of the "stiff/strong" matrix case. However, this conclusion is only true in absolute terms. In relative terms, the average 3-plet cluster height reaches saturation at a value of 75-80% of the axial cluster criterion, which was 330 µm and 78 µm for the "compliant/weak" and "stiff/strong" matrix case, respectively. This axial cluster criterion was setup based on the expected length over which the stress concentrations are significant, and is hence more or less proportional to the ineffective length in the three models.

The FEISM model was used to check how sensitive the cluster development is to the cluster criteria. These criteria (see section 4) essentially define a cylinder around each fibre break, within which all other fibre breaks are part of the same cluster. Figure 10 shows the effect of making this cylinder 50% larger by either increasing the axial or the radial criterion: the predicted number of individual fibre-breaks (i.e. unaffected by neighbouring breaks) and small clusters (up to 3-plets) decreased significantly, while the number of large broken clusters increased considerably; however, the predicted failure strain and corresponding fibre break density were only slightly affected by these changes in cluster criteria. Moreover, increasing the axial criterion by 50% increased the average 3-plet cluster height and standard deviation at the failure strain by about 40% for all cases, whereas they remained nearly the same when the radial criterion was increased by 50% (see Figure 10).

The above points illustrate that most cluster-related results (see Figure 5-Figure 8) are affected by the selected cluster criterion. The corresponding effect on the predicted failure strain depends on how each individual model deals with clusters and their associated stress concentrations, but it should be either zero in models which rely on equilibrium, such as DYSEM, or small in models which rely on non-linear superposition, such as 3PFM and FEISM. The plateau observed in the cluster height and standard deviation (see Figure 8) is likely to be an artefact of the fixed-distance criteria used. A criterion that is not based on a fixed distance would have been better, such as the one

based on a certain percentage of stress concentration proposed by Mesquita et al. [42] or based on recovery lengths as the one intrinsically built in HSL. However, such criteria are more difficult to apply in a consistent manner in different models.

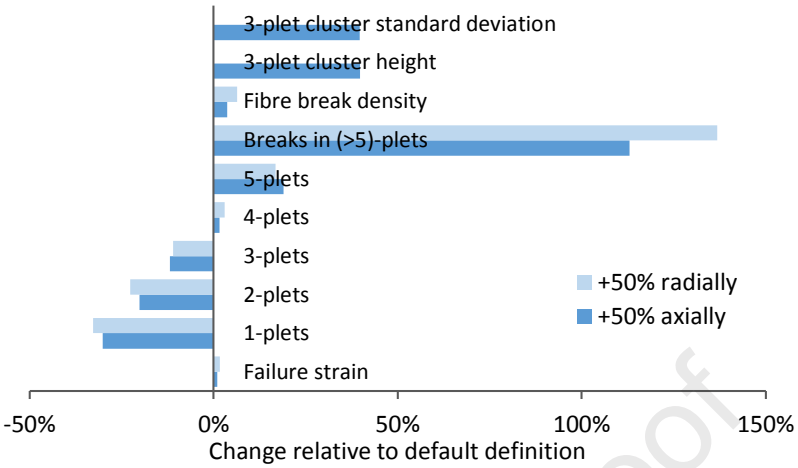

Figure 10: The change in failure strain, fibre break and cluster characteristics at the failure strain when the distance-based cluster criterion is extended to be 50% larger, as predicted by FEISM for the "stiff/strong" matrix case.

While the goal of this study was not to compare model predictions against experiments, it does seem that all three models predicting this feature (3PFM, DYSEM and FEISM) underestimate significantly the coplanarity levels observed experimentally [9]. This issue will likely need to be addressed in the future to allow reliable comparisons with experimental data.

7 Conclusions

Seven different models were compared with each other for the same set of input parameters, enabling an objective and blind comparison. The matrix properties were clearly shown to have an important effect on all model predictions. A stiffer and stronger matrix leads to increased composite strength and more localised stress concentrations, which in turn promote higher failure strains and strength, larger fibre break densities at the failure strain, smaller clusters and a lower degree of non-linearity in the stress-strain curve.

The FEISM, 3PFM and DYSEM models use relatively similar assumptions regarding stress redistributions around fibre breaks and cluster definition, and therefore predict similar failure strains, strengths, fibre breaks and cluster development. Nevertheless, the fastest of these three models (FEISM) is more than three orders of magnitude faster than the slowest (DYSEM). DFBM and GLS also share similar assumptions, and lead to

similar results. Owing to its different set of underlying assumptions regarding stress redistribution around fibre breaks and cluster definition, the HSL model yielded notably distinct results. Although its 2-plet development was faster, the differences only become pronounced closer to failure or for larger clusters. The cluster development in ABS was rather different from the other models, primarily due to its different cluster criterion and its rejection of strength values smaller than half of the mean fibre strength and larger than two standard deviations above the mean fibre strength.

The presented results identified clear drawbacks in the distance-based cluster criteria that were used. More objective criteria should be developed in the future, so that clustering of fibre breaks can be compared more objectively.

The next step in this benchmark is to compare the models against experimental data. This comparison is in preparation and will not be as blind as the present one, as a certain failure strain can be expected when the fibre type is known. However, it will extend the objective assessment of the model assumptions that was started in this paper.

8 Acknowledgements

This benchmark was performed within the framework of the FiBreMoD project and has received funding from the European Union's Horizon 2020 research and innovation programme under the Marie Skłodowska-Curie grant agreement No 722626. J.M. Guerrero would like to acknowledge the grant BES-2016-078270 from the 'Subprograma Estatal de Formación del MICINN' co-financed by the European Social Fund, and all authors from the University of Girona acknowledge the funding from the Spanish project RTI2018-097880-B-I00. The work of M. Hajikazemi forms part of the research programme of DPI, project 812T17. S. Pimenta acknowledges the funding from the Royal Academy of Engineering in the scope of her Research Fellowship on "Multiscale discontinuous composites for high-volume and sustainable applications" (2015-2019). The authors would also like to thank A.R. Bunsell, S. Joannès, J. Rojek, A. Thionnet, I. Sinclair, E. Schöberl, M.N. Mavrogordato and S.M. Spearing for their help in setting up the instructions for participants. R.P. Tavares and P.P. Camanho would like to thank the

financial support provided by FCT - Fundação para a Ciência e a Tecnologia through National Funds in the scope of project MITP-TB/PFM/0005/2013.

9 References

[1] Kaddour A, Hinton M, Smith P, Li S. *The background to the third world-wide failure exercise*. Journal of Composite Materials. 2013;47(20-21):2417-2426.

[2] Kaddour AS, Hinton MJ. *Maturity of 3D failure criteria for fibre-reinforced composites: Comparison between theories and experiments: Part B of WWFE-II*. Journal of Composite Materials. 2013;47(6-7):925-966.

[3] Kaddour AS, Hinton MJ, Smith PA, Li S. *A comparison between the predictive capability of matrix cracking, damage and failure criteria for fibre reinforced composite laminates: Part A of the third world-wide failure exercise*. Journal of Composite Materials. 2013;47(20-21):2749-2779.

[4] Rosen BW. *Tensile failure of fibrous composites*. AIAA Journal. 1964;2(11):1985-1991.

[5] Zweben C, Rosen BW. *A statistical theory of material strength with application to composite materials*. Journal of the Mechanics and Physics of Solids. 1970;18(3):189-206.

[6] Harlow DG, Phoenix SL. *The chain-of-bundles probability model for the strength of fibrous materials I: Analysis and conjectures*. Journal of Composite Materials. 1978;12(APR):195-214.

[7] Phoenix SL, Smith RL. *A comparison of probabilistic techniques for the strength of fibrous materials under local load-sharing among fibers*. International Journal of Solids and Structures. 1983;19(6):479-496.

[8] Fukuda H, Chou TW. *Monte Carlo simulation of the strength of hybrid composites*. Journal of Composite Materials. 1982;16(SEP):371-385.

[9] Swolfs Y, Morton H, Scott AE, Gorbatikh L, Reed PAS, Sinclair I, et al. *Synchrotron radiation computed tomography for experimental validation of a tensile strength model*

for unidirectional fibre-reinforced composites. Composites Part A: Applied Science and Manufacturing. 2015;77:106-113.

[10] Swolfs Y, Verpoest I, Gorbatikh L. *Issues in strength models for unidirectional fibre-reinforced composites related to Weibull distributions, fibre packings and boundary effects*. Composites Science and Technology. 2015;114:42-49.

[11] Swolfs Y, Verpoest I, Gorbatikh L. *Maximising the hybrid effect in unidirectional hybrid composites*. Materials & Design. 2016;93:39-45.

[12] Swolfs Y, McMeeking RM, Verpoest I, Gorbatikh L. *Matrix cracks around fibre breaks and their effect on stress redistribution and failure development in unidirectional composites*. Composites Science and Technology. 2015;108:16-22.

[13] Pimenta S. *A computationally-efficient hierarchical scaling law to predict damage accumulation in composite fibre-bundles*. Composites Science and Technology. 2017;146:210-225.

[14] Pimenta S, Pinho ST. *Hierarchical scaling law for the strength of composite fibre bundles*. Journal of the Mechanics and Physics of Solids. 2013;61(6):1337-1356.

[15] Guerrero JM, Tavares RP, Otero F, Mayugo JA, Costa J, Turon A, et al. *An analytical model to predict stress fields around broken fibres and their effect on the longitudinal failure of hybrid composites*. Composite Structures. 2019;211:564-576.

[16] Guerrero JM, Mayugo JA, Costa J, Turon A. *A 3D Progressive Failure Model for predicting pseudo-ductility in hybrid unidirectional composite materials under fibre tensile loading*. Composites Part A: Applied Science and Manufacturing. 2018;107:579-591.

[17] Tavares RP, Otero F, Turon A, Camanho PP. *Effective simulation of the mechanics of longitudinal tensile failure of unidirectional polymer composites*. International Journal of Fracture. 2017;208:269-285.

[18] Tavares RP, Otero F, Baiges J, Turon A, Camanho PP. *A dynamic spring element model for the prediction of longitudinal failure of polymer composites*. Computational Materials Science. 2019;160:42-52.

[19] Tavares RP, Melro AR, Bessa MA, Turon A, Liu WK, Camanho PP. *Mechanics of hybrid polymer composites: analytical and computational study*. Computational Mechanics. 2016;57:405-421.

[20] Swolfs Y, Verpoest I, Gorbatikh L. *A review of input data and modelling assumptions in longitudinal strength models for unidirectional fibre-reinforced composites*. Composite Structures. 2016;150:153-172.

[21] Scott AE, Sinclair I, Spearing SM, Thionnet A, Bunsell AR. *Damage accumulation in a carbon/epoxy composite: Comparison between a multiscale model and computed tomography experimental results*. Composites Part A: Applied Science and Manufacturing. 2012;43(9):1514-1522.

[22] de Morais AB. *Prediction of the longitudinal tensile strength of polymer matrix composites*. Composites Science and Technology. 2006;66(15):2990-2996.

[23] Hui CY, Phoenix SL, Ibnabdeljalil M, Smith RL. *An exact closed form solution for fragmentation of Weibull fibers in a single filament composite with applications to fiber-reinforced ceramics*. Journal of the Mechanics and Physics of Solids. 1995;43(10):1551-1585.

[24] Jonas E, Schulz-Hardt S, Frey D, Thelen N. *Confirmation bias in sequential information search after preliminary decisions: An expansion of dissonance theoretical research on selective exposure to information*. Journal of Personality and Social Psychology. 2001;80(4):557-571.

[25] Swolfs Y, McMeeking RM, Rajan VP, Zok FW, Verpoest I, Gorbatikh L. *Global load sharing model for unidirectional hybrid fibre-reinforced composites*. Journal of the Mechanics and Physics of Solids. 2015;84:380-394.

[26] Feih S, Mouritz AP. *Tensile properties of carbon fibres and carbon fibre–polymer composites in fire*. Composites Part A: Applied Science and Manufacturing. 2012;43(5):765-772.

[27] Xiao H, Lu Y, Wang M, Qin X, Zhao W, Duan J. *Effect of gamma-irradiation on the mechanical properties of polyacrylonitrile-based carbon fiber*. Carbon. 2013;52:427-439.

[28] Deng S, Ye L, Mai Y-W, Liu H-Y. *Evaluation of fibre tensile strength and fibre/matrix adhesion using single fibre fragmentation tests*. Composites Part A: Applied Science and Manufacturing. 1998;29(4):423-434.

[29] Mesquita F, Swolfs Y, Bucknell S, Leray Y, Lomov SV, Gorbatikh L, *Tensile properties of single carbon fibres tested with automated equipment*, 22nd International Conference on Composite Materials, Melbourne, Australia, 2019.

[30] Joannès S, Islam F, Laiarinandrasana L. *Uncertainty in fibre strength characterisation due to uncertainty in measurement and sampling randomness*. Applied Composite Materials. 2020;27:165-184.

[31] Islam F. *Probabilistic single fibre characterisation to improve stochastic strength modelling of unidirectional composites* PhD thesis. Mines ParisTech, 2020.

[32] Islam F, Joannès S, Bucknell S, Leray Y, Bunsell A, Laiarinandrasana L. *Investigation of tensile strength and dimensional variation of T700 carbon fibres using an improved experimental setup*. Journal of Reinforced Plastics and Composites. 2020;39(3-4):144-162.

[33] Bunsell A, Gorbatikh L, Morton H, Pimenta S, Sinclair I, Spearing M, et al. *Benchmarking of strength models for unidirectional composites under longitudinal tension*. Composites Part A: Applied Science and Manufacturing. 2018;111:138-150.

[34] Breite C, Gorbatikh L, Swolfs Y, Alves M, Pimenta S, Schöberl E, et al., *Benchmarking exercise II for longitudinal strength models of unidirectional composites - Instructions for participants, www.fibremodproject.eu*, FiBreMoD European Training Network, June 2020.

[35] McCartney LN. *Analytical Models for Sliding Interfaces Associated with Fibre Fractures or Matrix Cracks*. Computers, Materials & Continua. 2013;35(3):183-227.

[36] McCartney LN. *Simulation of progressive fiber failure during the tensile loading of unidirectional composites*. NPL report CMMT(A)212: National Physical Laboratory, UK; 1999.

[37] Okabe T, Ishii K, Nishikawa M, Takeda N. *Prediction of Tensile Strength of Unidirectional CFRP Composites*. Advanced Composite Materials. 2010;19(3):229-241.

[38] Guerrero JM, Mayugo JA, Costa J, Turon A. *Failure of hybrid composites under longitudinal tension: Influence of dynamic effects and thermal residual stresses*. Composite Structures. 2020;233:111732.

[39] McCartney LN. *Physically based damage models for laminated composites*. Proceedings of the Institution of Mechanical Engineers, Part L: Journal of Materials: Design and Applications. 2003;217(3):163-199.

[40] St-Pierre L, Martorell NJ, Pinho ST. *Stress redistribution around clusters of broken fibres in a composite*. Composite Structures. 2017;168:226-233.

[41] Beyerlein IJ, Phoenix SL. *Stress concentrations around multiple fiber breaks in an elastic matrix with local yielding or debonding using quadratic influence superposition*. Journal of the Mechanics and Physics of Solids. 1996;44(12):1997-2039.

[42] Mesquita F, Swolfs Y, Lomov SV, Gorbatikh L. *Ply fragmentation in unidirectional hybrid composites linked to stochastic fibre behaviour: A dual-scale model*. Composites Science and Technology. 2019;181:107702.

Declaration of interests

☒ The authors declare that they have no known competing financial interests or personal relationships that could have appeared to influence the work reported in this paper.

☐The authors declare the following financial interests/personal relationships which may be considered as potential competing interests: